

Supplementary Information

Superior Spin-Polarized Electronic Structure in MoS₂/MnO₂ Heterostructures with An Efficient Hole Injection

Baozeng Zhou*, Zheng Li, Jiaming Wang, Kangqiang Wang

*Tianjin Key Laboratory of Film Electronic & Communicate Devices, School of Electrical and
Electronic Engineering, Tianjin University of Technology, Tianjin 300384, China*

*Author to whom all correspondence should be addressed.

E-mail: baozeng@tju.edu.cn

Table S1. Calculated lattice constant a , M - X bond length (d_{M-X}), layer thickness (d_{X-X}), interlayer distance D , energy difference (ΔE) between FM and AFM states, magnetic moments (Mag), and work function (Φ) of the pristine monolayers and the most stable most stable configurations in each group.

	a (Å)	d_{M-X} (Å)	d_{X-X} (Å)	D (Å)	ΔE (meV)	Mag (μ_B)	Φ (eV)
h -MnO ₂	2.90	1.85	2.31	–	38	0.66	6.31
t -MnO ₂	2.98	1.88	2.50	–	53	3.00	6.98
MoS ₂	3.13	2.37	3.12	–	–	0.00	5.85
MoS ₂ / h MnO ₂	3.05	–	–	2.79	45	1.20	5.96
MoS ₂ / t MnO ₂	3.06	–	–	2.76	49	3.00	6.32

Table S2. In-plane lattice constant a , equilibrium interlayer distance D , and binding energies (E_b) of all stacking models.

MoS ₂ / <i>h</i> -MnO ₂	AA	AB	C27	C28	T1	T2
a (Å)	3.05	3.05	3.03	3.05	3.06	3.05
D (Å)	3.21	2.79	2.86	3.18	2.83	2.80
E_b (meV)	-133.7	-296.5	-239.2	-138.3	-221.7	-243.6
MoS ₂ / <i>t</i> -MnO ₂	fcc-I	fcc-II	hcp-I	hcp-II	top-I	top-II
a (Å)	3.06	3.06	3.05	3.06	3.06	3.06
D (Å)	2.80	2.76	2.82	2.86	3.29	3.27
E_b (meV)	-312.3	-337.8	-309.2	-303.7	-180.7	-188.6

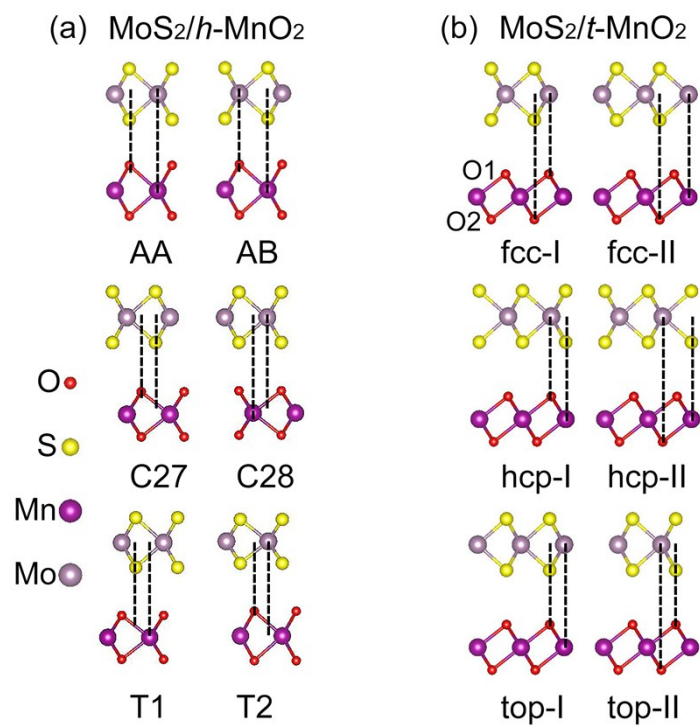


Fig. S1. Side views of the nonequivalent configurations of (a) $\text{MoS}_2/h\text{-MnO}_2$ and (b) $\text{MoS}_2/t\text{-MnO}_2$ heterostructures.

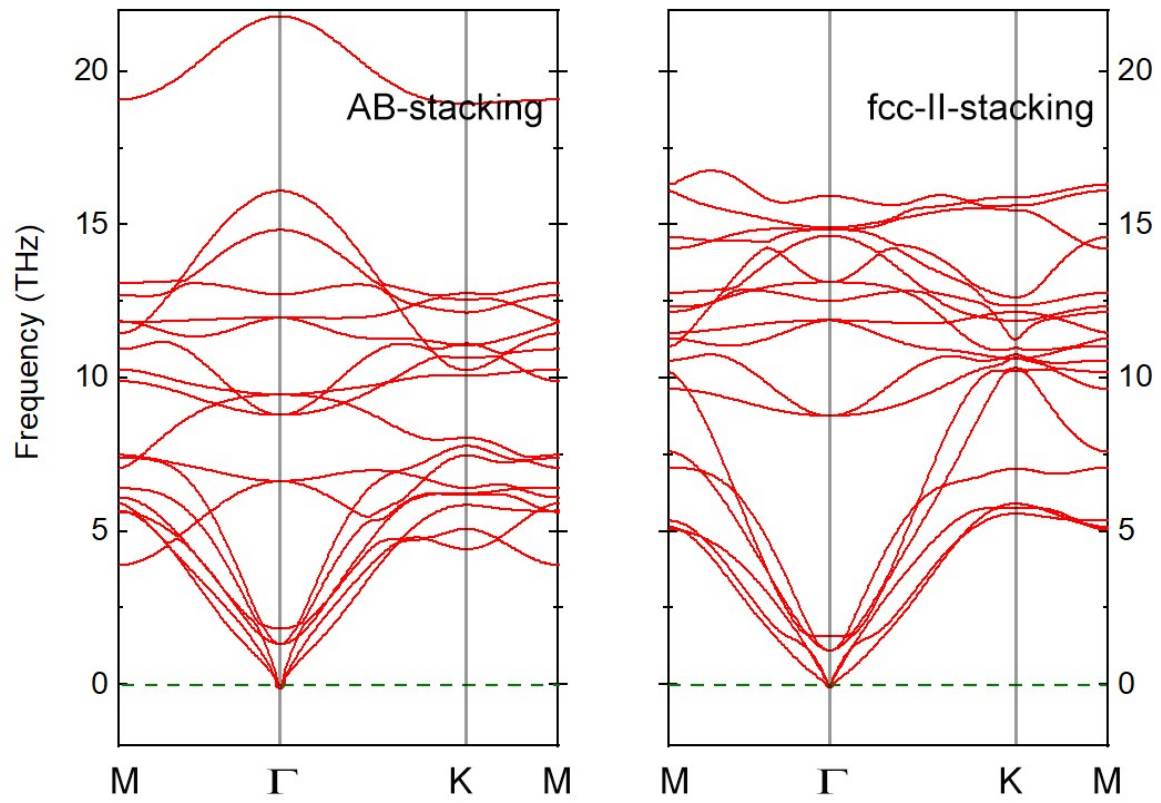


Fig. S2. Phonon bands of AB and fcc-II stacking models.

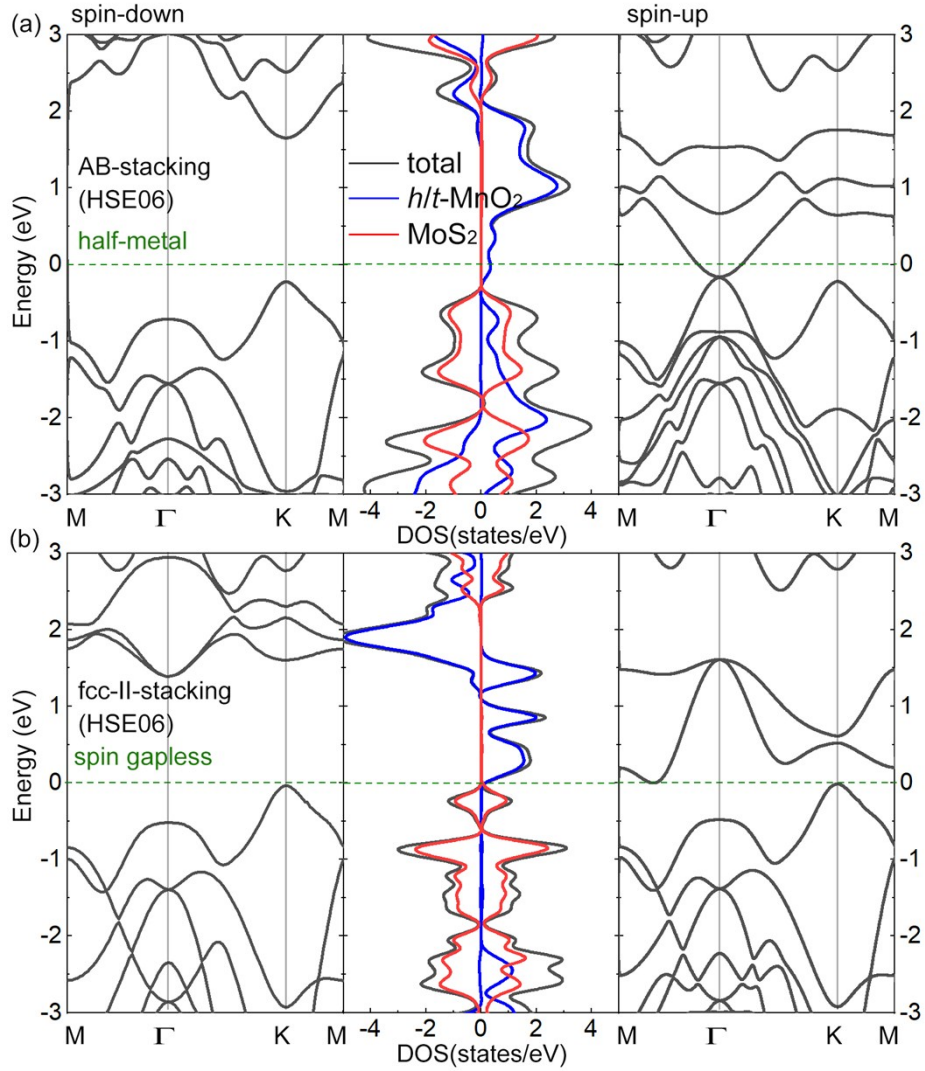


Fig. S3. The calculated band structures and DOS by HSE06 methods for (a) AB and (b) fcc-II stacking heterostructures, respectively. The Fermi levels are set to zero.

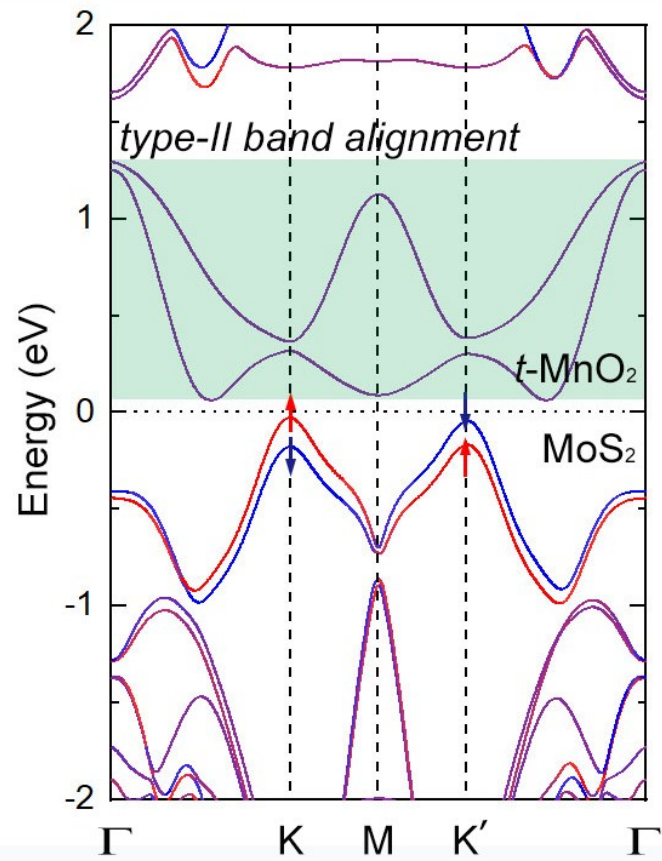


Fig. S4. Valley polarization in MoS₂/t-MnO₂ heterostructure. Spin-up and spin-down states are presented by red and blue, respectively.

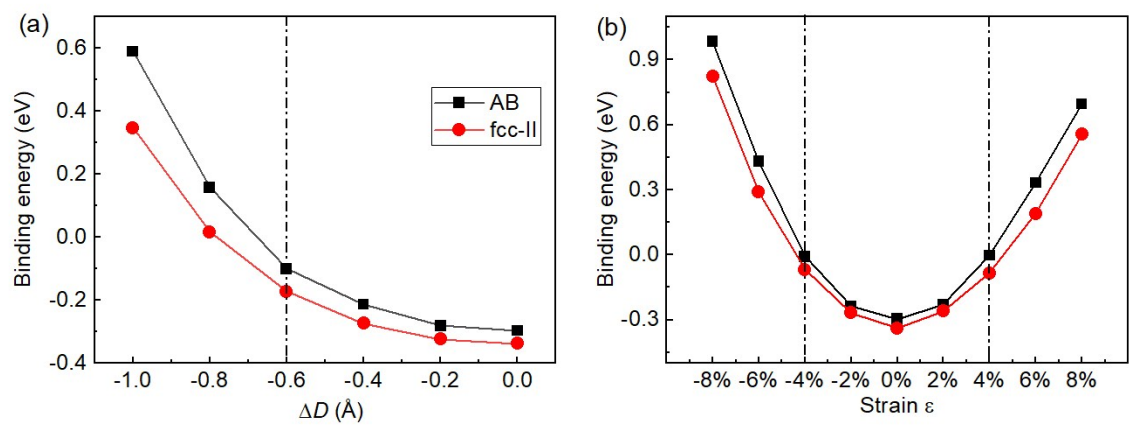


Fig. S5. Binding energies per unit cell as a function of (a) the interlayer distance and (b) in-plane strain in AB and fcc-II stacking heterostructures.

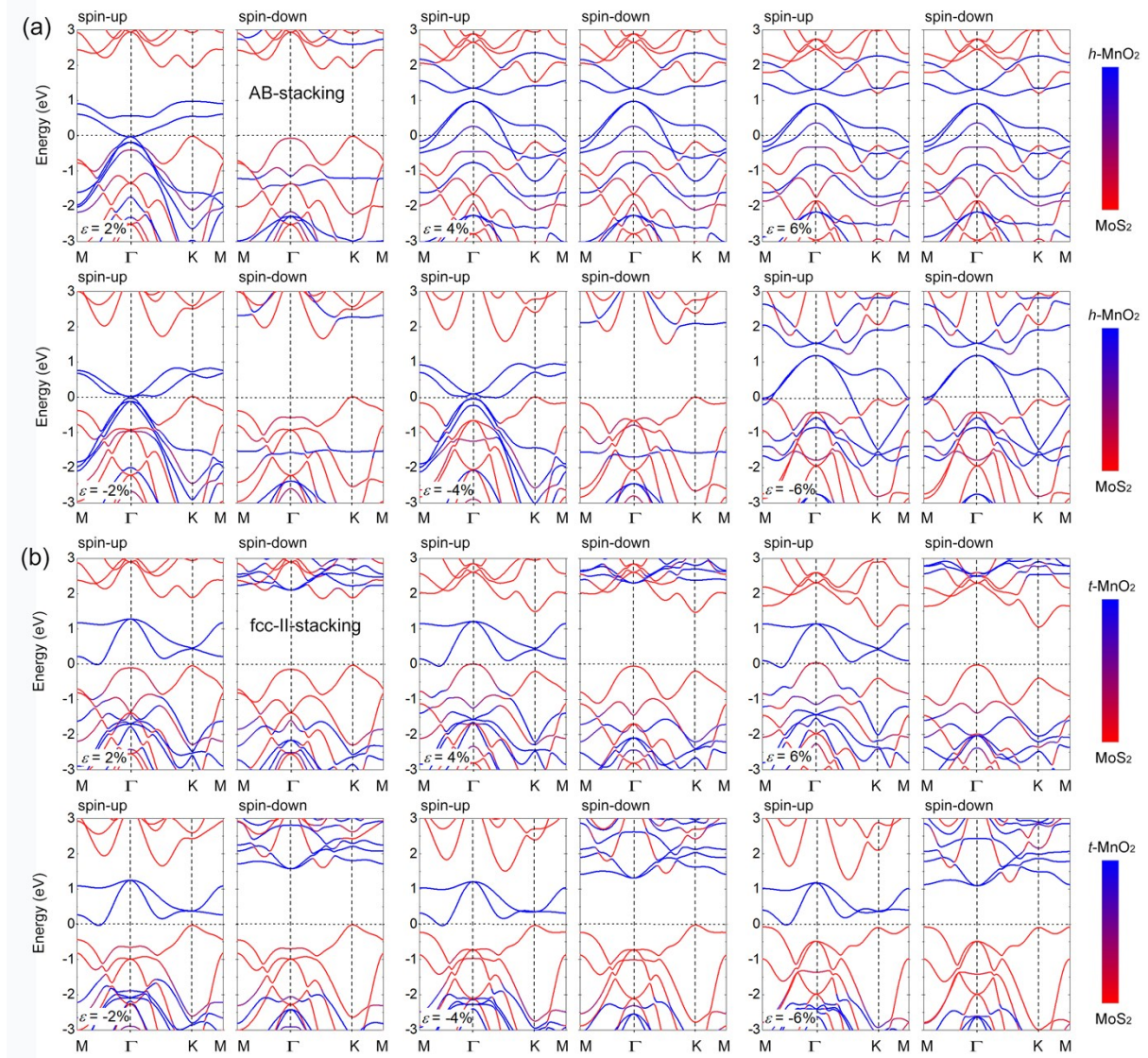


Fig. S6. Band structures of (a) AB-stacking and (b) fcc-II stacking models with varying in-plane biaxial strain. The Fermi level is set to zero.